



Title	A kinematically reasonable mechanism of tongue forward protrusion considering hyoid bone movements
Author(s)	Inoue, Kyoichi; Otani, Tomohiro; Nozaki, Kazunori et al.
Citation	Journal of Biomechanics. 2025, 178, p. 112445
Version Type	VoR
URL	https://hdl.handle.net/11094/98563
rights	This article is licensed under a Creative Commons Attribution 4.0 International License.
Note	

The University of Osaka Institutional Knowledge Archive : OUKA

<https://ir.library.osaka-u.ac.jp/>

The University of Osaka



A kinematically reasonable mechanism of tongue forward protrusion considering hyoid bone movements

Kyoichi Inoue ^a, Tomohiro Otani ^{a,*}, Kazunori Nozaki ^b, Tsukasa Yoshinaga ^a, Shigeo Wada ^a

^a Graduate School of Engineering Science, Osaka University, 1-3 Machikaneyamacho, Toyonaka, Osaka 560-8531, Japan

^b Division for Medical Information, Osaka University Dental Hospital, 1-8 Yamadaoka, Suita, Osaka 565-0871, Japan

ARTICLE INFO

Keywords:

Tongue muscle
Genioglossus
Hyoid bone
Ultrasound imaging
Tongue kinematics
Finite element method

ABSTRACT

The tongue has a wide variety of motor functions, which are driven by tongue muscle contractions and associated with movements of the hyoid bone (HB) connected to the tongue root. HB movement has been observed in many situations, including swallowing, breathing, and speech. However, the relationships between HB movement and tongue kinematic function have received little attention, and have not been considered in most previous biomechanical tongue modeling research, except studies of swallowing. The current study aimed to clarify the effects of HB movement on tongue kinematics during tongue forward protrusion, which is an essential tongue motor function associated with speech disorder. HB displacement during tongue forward protrusion was quantified using ultrasound imaging in four healthy controls. Furthermore, computational mechanical simulations of tongue forward protrusion were conducted with observed HB movements and active contraction of the genioglossus (GG) muscle, which is conventionally considered to be the driving muscle in tongue forward protrusion. Ultrasound imaging revealed anterosuperior HB displacement in tongue forward protrusion, with a similar magnitude in each direction (anterior: 6.3 ± 2.8 mm, superior: 5.8 ± 1.6 mm). Computational simulation demonstrated that the HB movement described above caused not only anterosuperior displacement, but also forward rotation of the tongue body, which was caused by kinematic constraints of GG. The resulting anterior displacement of the tongue tip was 1.5 times greater compared with that without HB movement. These findings indicate that the HB and associated tongue body movements play non-negligible roles in the tongue kinematics of forward protrusion.

1. Introduction

The tongue consists of multiple muscles classified into four extrinsic and four intrinsic muscles (Abd-El-Malek, 1939; Takemoto, 2001) and exhibits a variety of motor functions that play essential roles in daily life, including speech, swallowing, and respiration (Hiemae and Palmer, 2003). The tongue is fixed to the mandible by the genioglossus (GG), which is the largest extrinsic tongue muscle. The GG is oriented from the mental spine to the tongue body (Bailey, 2011; Doran and Baggett, 1971; Sanders and Mu, 2013), and attaches to the hyoid bone (HB) at the tongue root. Because the HB does not articulate with other bones, its position can be altered via flexible changes in the mechanical balance among suprathyroid and infrathyroid muscle forces (Pancherz et al., 1986), as observed during swallowing (Kim and McCullough, 2008; Yabunaka et al., 2011), neck flexion/extension (Zheng et al., 2012), jaw opening/

closing (Laboissière et al., 1996), and speech (Westbury, 1988). Therefore, tongue kinematics result not only tongue in muscle deformation but also translation- and rotation-associated HB movements (Ross et al., 2024).

However, associations between HB movements and tongue kinematics are unclear, and have received little research attention in the fields of tongue functional anatomy and oral biomechanics, except in studies of swallowing (e.g., (Ross et al., 2024). Recent computational biomechanical studies examined tongue motor function via active contraction and passive deformation of the tongue muscles, especially during speech production (Al-Zanoon et al., 2024; Buchaillard et al., 2007; Fujita et al., 2007; Gomez et al., 2020, 2018; Kappert et al., 2021; Koike et al., 2017; Stavness et al., 2012, 2011). However, to the best of our knowledge, except for one study by (Wu et al., 2014), previous studies were based on the simplifying assumption that the HB

* Corresponding author at: Department of Mechanical Science and Bioengineering, Graduate School of Engineering Science, Osaka University, 1-3 Machikaneyamacho, Toyonaka, Osaka 560-8531, Japan.

E-mail address: otani.tomohiro.es@osaka-u.ac.jp (T. Otani).

connecting the tongue root surface is fixed with no displacement or constrained by linear springs. Because this simplification involves the risk of inconsistent HB movements and overestimating tongue muscle deformation to account for experimentally observed tongue kinematics, the association with HB movements should be clarified to deepen our understanding of the mechanisms underlying tongue motor function.

From this perspective, the current study focused on tongue forward protrusion, which is an essential tongue motor function and is applied for exercises in voice therapy (Behrman and Haskell, 2008) because of its association with motor speech disorder (American Speech-Language-Hearing Association, n.d.). Tongue forward protrusion is conventionally understood to be driven by GG active contraction that shifts the tongue body toward the anterior direction, on the basis of muscle fiber orientation (Sanders and Mu, 2013) and electromyography (EMG) data (Pittman and Bailey, 2009; Webb and Adler, 2007). Following the understanding of the mechanism of forward protrusion described above, previous computational studies have attempted to express tongue forward protrusion mainly by GG active contractions (Koike et al., 2017; Stavness et al., 2012). However, these simulations have not considered actual HB movement because of a lack of experimental data, and the resulting tongue movements were small, approximately 10 mm of tongue tip anterior displacement even considering not only GG but also other intrinsic tongue muscles.

The current study aimed to clarify the effects of HB movements on tongue kinematics in tongue forward protrusion. We hypothesized that the HB movement is a non-negligible factor in determining the actual characteristics of tongue forward protrusion and performed *in vivo* measurements of HB displacements and computational simulations of the tongue forward protrusion considering HB movements. HB displacement during forward protrusion was evaluated using ultrasound imaging, which is a well-established noninvasive protocol for examining *in vivo* HB displacement (Kwan et al., 2014; Yabunaka et al., 2011). Subsequently, tongue kinematics during forward protrusion were computationally expressed using the method described in our previous study (Koike et al., 2017), by solving mechanical balances of active muscle contraction and elastic deformation of three-dimensional tongue geometry. The resulting tongue deformation states with and without HB movements were then compared.

2. Materials and Methods

2.1. Ultrasound imaging

Four healthy subjects (male, 20–25 years old) with no prior history of tongue disorders volunteered to participate in this study. The study was approved by the Institutional Review Board of Osaka University Dental Hospital (No. H30-E8-1). Ultrasound images were collected using an EPIQ7 ultrasound system (Philips, Amsterdam, the Netherlands) with a curved array mC12-3 PureWave transducer (8 MHz) for 10 repetitive trials of tongue forward protrusion in each subject. Measurements were conducted while subjects sat in an upright position, with their back resting against a wall to restrict head movement, following the protocol described by (Yabunaka et al., 2011). The target point for moving the tongue tip was located along the line passing the tragale and subnasale (on the Camper plane) on the midsagittal plane, and subjects were instructed to protrude their tongue with jaw opening toward the above target point within 3 s (Fig. 1[a]). The transducer was positioned submentally to obtain a lateral view, and was pointed at the posterior region of the tongue on the midsagittal plane, in accord with (Kwan et al., 2014). Ultrasound images with a depth of 60 mm and spatial distributions of $112 \times 84 \text{ mm}^2$ were recorded at 30 frames per second (fps). In addition, a video camera (HDR-CX470, SONY, Tokyo, Japan) was placed to the left of the subject, and videos were recorded at 30 fps to confirm the correctness of the above alignments and measure the displacements of the tongue tip and handheld transducer.

HB displacement in the anterior-posterior and superior-inferior

directions was quantified from the ultrasound images. In the ultrasound images, the HB was identified on the scan with a posterior acoustic shadow and the measurement point of the HB was set on the tip of the cranial HB (Fig. 1b), following the method described by (Yabunaka et al., 2011). Measurement point tracking in ultrasound images during tongue protrusion was conducted using the optical flow algorithm implemented in OpenCV library (<https://opencv.org/>) and the HB trajectory in the ultrasound image was obtained (Fig. 1[c]). To assess HB displacement along each body axis (anterior-posterior and superior-inferior directions), the HB trajectory recorded in the local coordinates of the ultrasound images was transformed to global coordinates (body coordinates). Because the local coordinates in the ultrasound images can be identified from the position and direction of the transducer, we placed a rectangular marker (width: 4.2 mm and height: 25 mm) along the central axis of the transducer (Fig. 1[a]) and the local coordinates were detected from snapshots of the movie taken from the left side of the subject at the corresponding time of the ultrasound images.

The tongue tip displacement during tongue forward protrusion was evaluated from the video acquired from the camera. The measurement point was set on the tongue tip and this trajectory during the tongue forward protrusion was extracted using the same method of HB displacement measurement described above.

2.2. Computational simulation

Three-dimensional geometries of the tongue and surrounding mandible and HB were reconstructed from computed tomography (CT) images acquired in our previous study (Koike et al., 2017), which were volumetric images of speech organs of a 42-year-old male subject in a resting position (jaw closed) with a voxel size of $0.488 \times 0.488 \times 0.5 \text{ mm}^3$. The tongue, mandible, and HB were extracted from CT images using Mimics 24.0 (Materialise Inc, Yokohama, Japan), as shown in Fig. 2(a), and a tetrahedral volumetric mesh of 109,898 elements of the tongue was created by hyperMesh (Altair Engineering Inc., Troy, MI). The reconstructed tongue domain was divided into the tongue body, GG, and geniohyoid (GH) connecting the inner mandible and HB, in accord with (Sanders and Mu, 2013) (Fig. 2[b]). The muscle fiber orientation in GG and GH was expressed as a spatially continuous function of the unit vector \mathbf{a}_0 at the initial state obtained from the solution of the Laplace equation (Gomez et al., 2018; Otani et al., 2020) (Fig. 2[c]). To express tongue forward protrusion, as observed in ultrasound images, we considered the jaw opening posture of both the tongue and surrounding bones by rigid rotation in sagittal planes around the mandibular condyle with an angle of 15° (Muto and Kanazawa, 1994).

Mechanical balance states of the tongue were obtained by solving the static equilibrium equation. Muscles were represented using a continuum model applied in (Koike et al., 2017) (see electronic supplementary material 1 for details), which is inspired from a Hill model consisting of the parallel active contractions and passive elasticity, as in the general continuum model of muscles (Dao and Tho, 2018). The elastic properties of the tongue were expressed by a nearly incompressible hyperelastic material applied in (Buchailard et al., 2009; Koike et al., 2017). The strain elastic energy density function was set as a 5-parameter Mooney-Rivlin law with $c_{10} = 1,037 \text{ Pa}$, $c_{20} = 486 \text{ Pa}$, and $c_{01} = c_{11} = c_{02} = 0 \text{ Pa}$ (Buchailard et al., 2009) and the bulk modulus in the volumetric component was set to 2,000 Pa (Koike et al., 2017). The active contraction force of the muscle was set to 2,000 Pa in GG (Koike et al., 2017) and zero in GH. Although the GH contraction works on the HB movements, this study set the HB movement to be prescribed from the ultrasound imaging, and thus did not consider the GH active contraction (for the case with GH active contraction, see electronic supplementary material 2). Regarding boundary conditions, a fixed displacement boundary condition was set on the attachment surface to the mandible and HB. Here, the HB forward rotation of 20° on the sagittal plane was considered to constitute a reasonable range, in accord with (Westbury, 1988).

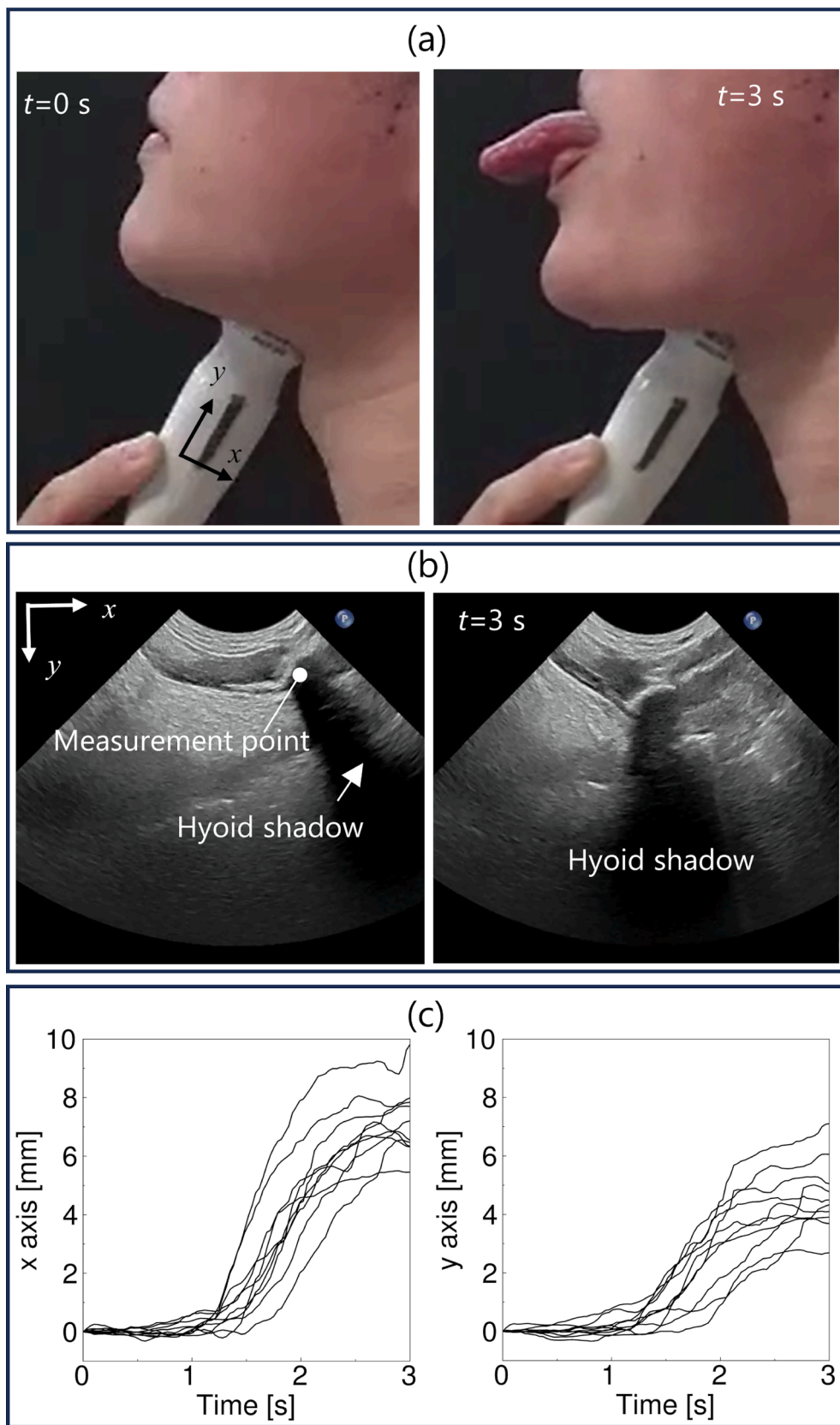


Fig. 1. Ultrasound imaging of hyoid bone (HB) during tongue forward protrusion. Position and displacement of the transducer and the tongue tip were recorded by video camera located on the left side of the subject (a). The HB position was identified from the tip of the hyoid shadow (b) and its trajectory was tracked (c) in the local coordinates of the ultrasound images shown in the x and y axes.

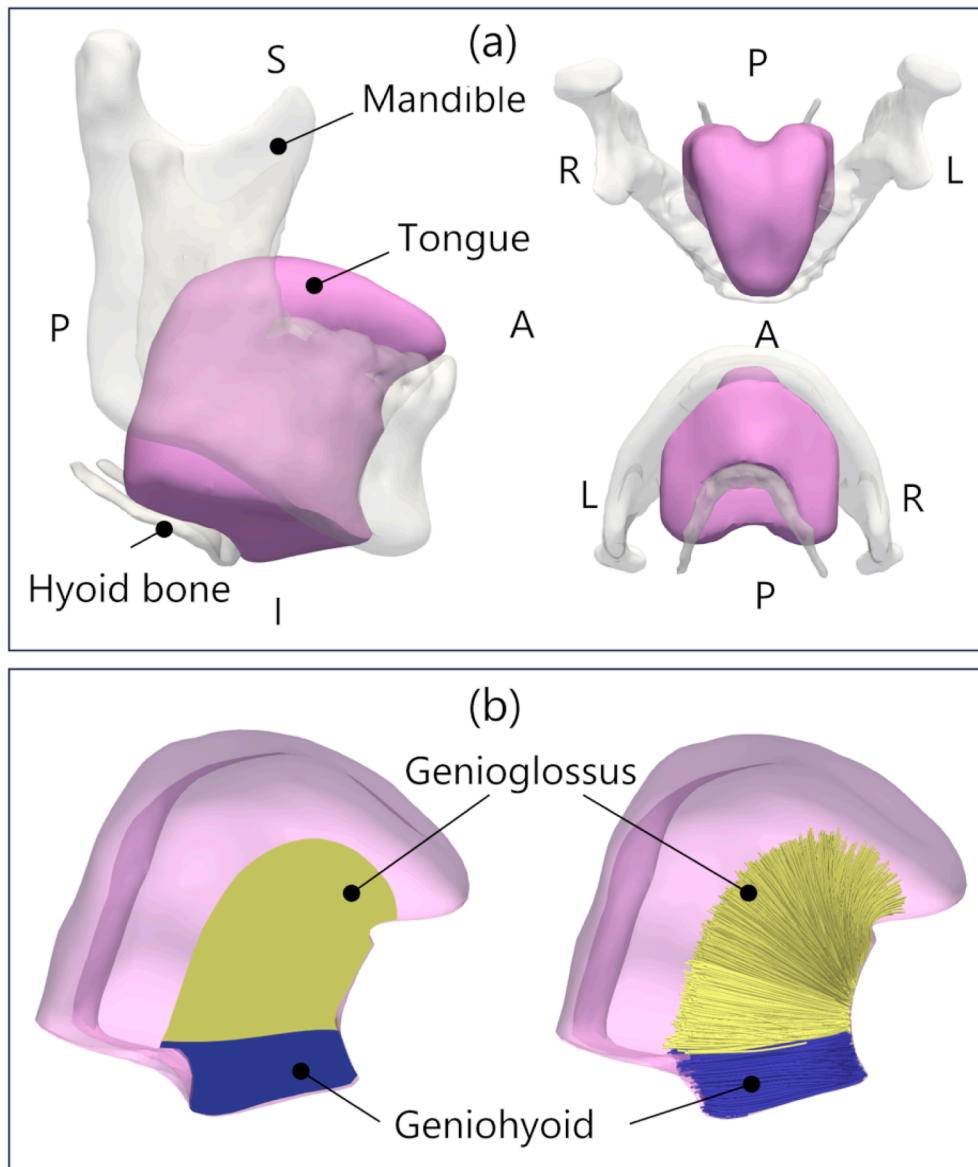


Fig. 2. (a) Reconstructed geometries of the tongue and surrounding mandible and hyoid bone (HB). The tongue domain was divided into three parts: tongue body, genioglossus (GG), and geniohyoid (GH). (b) Muscle fiber orientations in GG and GH were expressed as continuous form using the method described by (Gomez et al., 2018).

Computational simulations were conducted using an in-house finite element method solver and the linear algebraic equation was solved using PARDISO implemented in the Intel oneAPI Math Kernel Library. We conducted two computational examples with and without HB displacement on the basis of ultrasound imaging, and compared the resulting tongue deformation states. To assess the characteristics of the resulting tongue movements, we utilized three evaluation indices. First, for the GG and GH, rotations of these muscles and the associated tongue body were evaluated by the muscle fiber rotation angle θ in the mid-sagittal plane, given by

$$\theta = \cos^{-1}(\mathbf{a}_0 \cdot \mathbf{a} / |\mathbf{a}_0| |\mathbf{a}|) \quad (1)$$

where \mathbf{a} is the unit vector directing the muscle fiber orientation at the current state. Second, equivalent strain distribution in the tongue was computed to confirm the deformation states mainly in the tongue body caused by GG contractions and HB movements. Here, the equivalent strain was computed from the Green-Lagrange strain tensor. Third, muscle fiber deformation states in the GG and GH were evaluated by the

fiber stretch ratio λ , given by

$$\lambda = \sqrt{\mathbf{a}_0^\top \cdot \bar{\mathbf{C}} \cdot \mathbf{a}_0} \quad (2)$$

where $\bar{\mathbf{C}} = J^{-\frac{2}{3}} \mathbf{C}$, \mathbf{C} is the right Cauchy-Green deformation tensor, and J is the volume change ratio.

3. Results

3.1. Ultrasound imaging

The HB exhibited translation in the anterior and superior directions, and the degree of displacement was within a comparable range in each subject, with an average displacement of 6.3 ± 2.8 mm in the anterior direction and 5.8 ± 1.6 mm in the superior direction. In contrast, the tongue tip mainly exhibited translation in the anterior direction, and slightly shifted in the inferior direction in each subject. The average anterior displacement of the tongue tip was 23.9 ± 3.9 mm whereas the

average superior displacement was -4.8 ± 6.2 mm. Each subject data is summarized in Table 1.

3.2. Computational simulation

Computational simulations of tongue forward protrusion were performed with/without considering HB displacement, with both anterior and superior displacements of 6 mm, considering the reasonable range observed in the ultrasound imaging described above.

In the case with HB displacement, the tongue root was translated to the anterosuperior direction and caused forward rotations of GG and GH (Fig. 3(a) left). The degree of the forward rotation angle was 10–20° in the GH and GG lower (horizontal) region and locally exceeded 30° in the GG upper (oblique) region (Fig. 3(b) left). The resulting anterior displacement of the tongue tip was 18.5 mm. In contrast, the case without HB displacement also showed anteroinferior displacement of the tongue tip, but the magnitude was relatively small (anterior displacement: 12.1 mm) (Fig. 3(a) right). The forward fiber rotation was lower than 5° in almost all domains, except for the upper region of the GG (Fig. 3(b) right).

In contrast, the volume fraction of the equivalent strain in the midsagittal plane of the tongue after forward protrusion showed similar profiles regardless of HB displacement (Fig. 4). In both cases, the strain in the tongue body was almost zero; thus, the tongue body motion exhibited rigid-like translation and rotation. The strain distribution in the GG region was almost constant, except for the boundaries of the mental spine.

Muscle fiber deformation after the tongue forward protrusion showed different tendencies, especially in GH due to HB displacement (Fig. 5). The GG muscle fibers were contracted in almost all regions (stretch ratio < 1) except for the region near the inner mandible, and these distributions were comparable regardless of HB displacement. In contrast, GH muscle fiber deformation was not observed in the case without HB displacement, whereas GH fibers were contracted in almost all regions in the case with HB displacement. Regarding the volume fraction of the fiber stretch ratio, the degree of fiber stretch in the GG region was moderate in the case with HB displacement, whereas fiber stretch in the GH region exhibited a stretch ratio of less than 1.

4. Discussion

Although HB movement in oral motor control has been widely studied, its relationship to tongue kinematics is not well understood. Thus, we hypothesized that HB movements play a non-negligible role in actual tongue kinematics, and investigated the effects of HB movement in tongue forward protrusion, as one of the fundamental motor functions of the tongue. Actual HB movement and displacement were quantified using ultrasound imaging, which is an established technique for tracking HB motion in a non-invasive way (Kwan et al., 2014; Yabunaka et al., 2011). Furthermore, computational simulations of tongue forward

protrusion were performed not only with active GG contraction, which is conventionally understood as a driving force (Bailey, 2011; Sanders and Mu, 2013), but also with HB movement, and the kinematic implications of HB movement were evaluated. The current results successfully demonstrated characteristic HB movement during tongue forward protrusion, and examined its contribution to the resulting tongue kinematics, as described below.

Ultrasound imaging of HB displacement in tongue forward protrusion revealed that HB translation was accompanied by tongue tip displacement. Although the tongue tip mainly exhibited translation in the anterior direction, the HB exhibited translation along not only the anterior but also the superior direction, in a comparable range regardless of subjects. Total displacements reached approximately 5–6 mm in each direction (Table 1). This magnitude of displacement is within the known range of displacement during swallowing (Yabunaka et al., 2011). Thus, we consider that the observed HB movements were within a physiologically reasonable range. Because the HB attaches to the tongue root, the current findings indicate that anterosuperior translation of the tongue body occurs during tongue forward protrusion.

To understand the implications of the phenomenon described above from the viewpoint of tongue kinematics, we further conducted a computational mechanical simulation of tongue forward protrusion with consideration of HB movements. The obtained results indicated that HB displacement shifted the tongue body in the anterosuperior direction, then caused the tongue body to rotate forward (Fig. 3) with slight tongue deformation (Fig. 4). Here, GG (especially the upper region) worked to limit the superior displacement of the tongue body with HB and led to the formation of this forward rotation. This complementary work of the upper region of GG is consistent with conventional anatomical knowledge (Sanders and Mu, 2013). As a result, the rigid-like tongue movement increased the magnitude of forward tongue protrusion and increased the anterior tongue tip deformation by 1.5 times, compared with that without HB movement. These results confirm that HB movement plays an important role in the kinematic mechanism of tongue forward protrusion, suggesting that the kinematic mechanism of tongue forward protrusion is not simple anterior displacement of the tongue body caused by GG contraction, but a combination of tongue muscle deformation and rigid-like tongue body motion associated with HB movement.

The HB movement described above is caused by changing the mechanical balance of the suprathyroid and infrathyroid muscle groups. In the current study, a computational simulation suggested that the GH contraction appeared along the muscle fiber orientation associated with HB movement (Fig. 5). These results support the kinematic reasonability of the HB movements observed in ultrasound imaging associated with GH contraction. The contribution of HB movements (*i.e.*, surrounding muscle groups) on tongue forward protrusion has the following clinical implications. Tongue forward protrusion is a widely used training modality for motor speech disorders and its effectiveness has been empirically verified (Behrman and Haskell, 2008), although the mechanism underlying its therapeutic efficacy remains unclear. The current results indicate that tongue forward protrusion is caused by not only tongue muscle contractions but also the HB movements driven by the supra- and infrathyroid muscle groups. Based on this finding, the tongue forward protrusion training could be interpreted to improve the above multiple muscle functions, associating with the HB position and mobility. Because inappropriate tongue position in the resting state is a known factor in speech disorder (American Speech-Language-Hearing Association, n.d.), the current results support the important role of the supra and infrathyroid muscle groups and their association with HB displacement in speech disorders.

The current study involved four main limitations that require further consideration. First, ultrasound imaging cannot detect the outline shape of the HB, and, in the current study, we were unable to examine HB rotation directly. In addition, HB and tongue tip displacement were measured using ultrasound imaging and video camera recording,

Table 1
Displacement of the hyoid bone and tongue tip (mean \pm S.D.) by tongue forward protrusion (mm).

	Hyoid bone		Tongue tip	
	Anterior direction	Superior direction	Anterior direction	Superior direction
Subject 1	10.1 ± 3.3	4.0 ± 2.2	26.0 ± 1.2	-2.3 ± 3.8
Subject 2	3.6 ± 1.4	5.0 ± 1.7	28.2 ± 1.7	-14.0 ± 2.6
Subject 3	5.5 ± 1.2	6.8 ± 1.7	21.5 ± 2.8	-1.3 ± 4.3
Subject 4	5.9 ± 0.7	7.3 ± 2.2	19.9 ± 3.1	-1.4 ± 3.1
All	6.3 ± 2.8	5.8 ± 1.6	23.9 ± 3.9	-4.8 ± 6.2

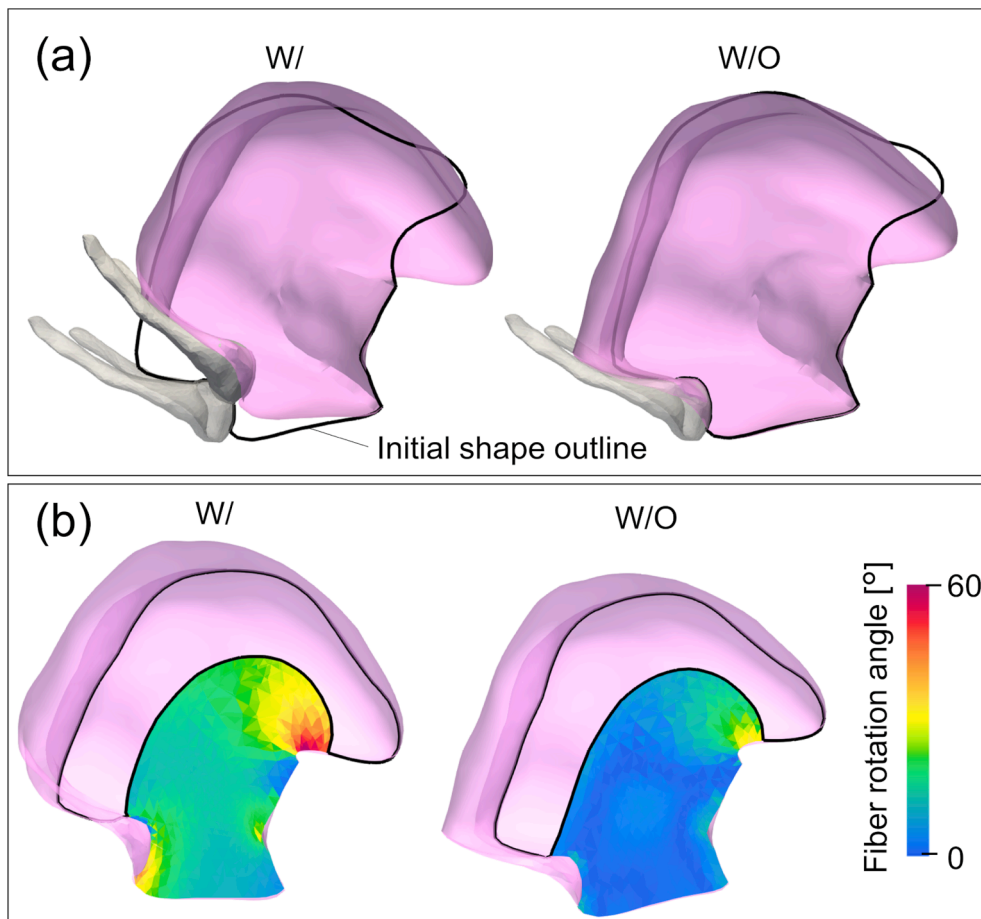


Fig. 3. Resulting deformed geometries of the tongue after forward protrusion (a) and spatial distribution of muscle fiber rotation angle on the mid-sagittal plane (b) with and without hyoid bone movements.

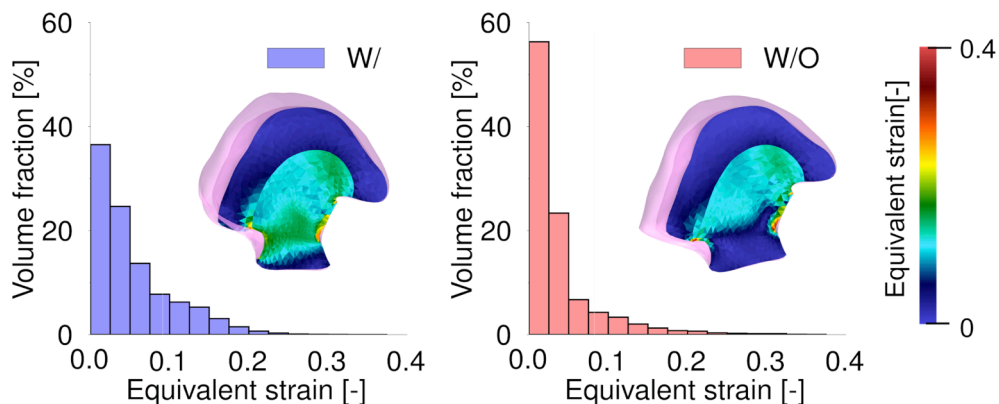


Fig. 4. Volume fractions of the equivalent strain in the tongue body after the forward protrusion with (left) and without (right) hyoid bone movements with these spatial distributions on the midsagittal plane.

respectively; thus, the synchronization could potentially have been affected by time-lags caused by hardware-dependent errors. Although X-ray videofluoroscopy is a well-established tool for measuring HB movement in dysphagia patients (Wei et al., 2022), measurements for healthy controls involve ethical issues because of their invasiveness. Further consideration of HB measurement using other modalities, such as dynamic magnetic resonance imaging (Moerman et al., 2012), may be a helpful next step. Second, this study included a small number of subjects, all of whom were healthy and young. Although this limitation may not be critical for examining the feasibility of the proposed role of

tongue kinematics in forward protrusion, large population studies examining age, sex, and prior history of oral diseases, especially speech disorders, may provide valuable insight into the clinical diagnosis of tongue motor dysfunction. Third, the computational simulation considered active contractions of the GG only, and the tongue body was assumed to constitute passive elastic material. Although it is commonly known that the GG is the main driving factor causing forward protrusion, intrinsic muscles in the tongue body also work to elongate the tongue body to produce forward protrusion as a muscular hydrostat (Kier, 2012) and to support the tongue posture to direct the tongue tip in

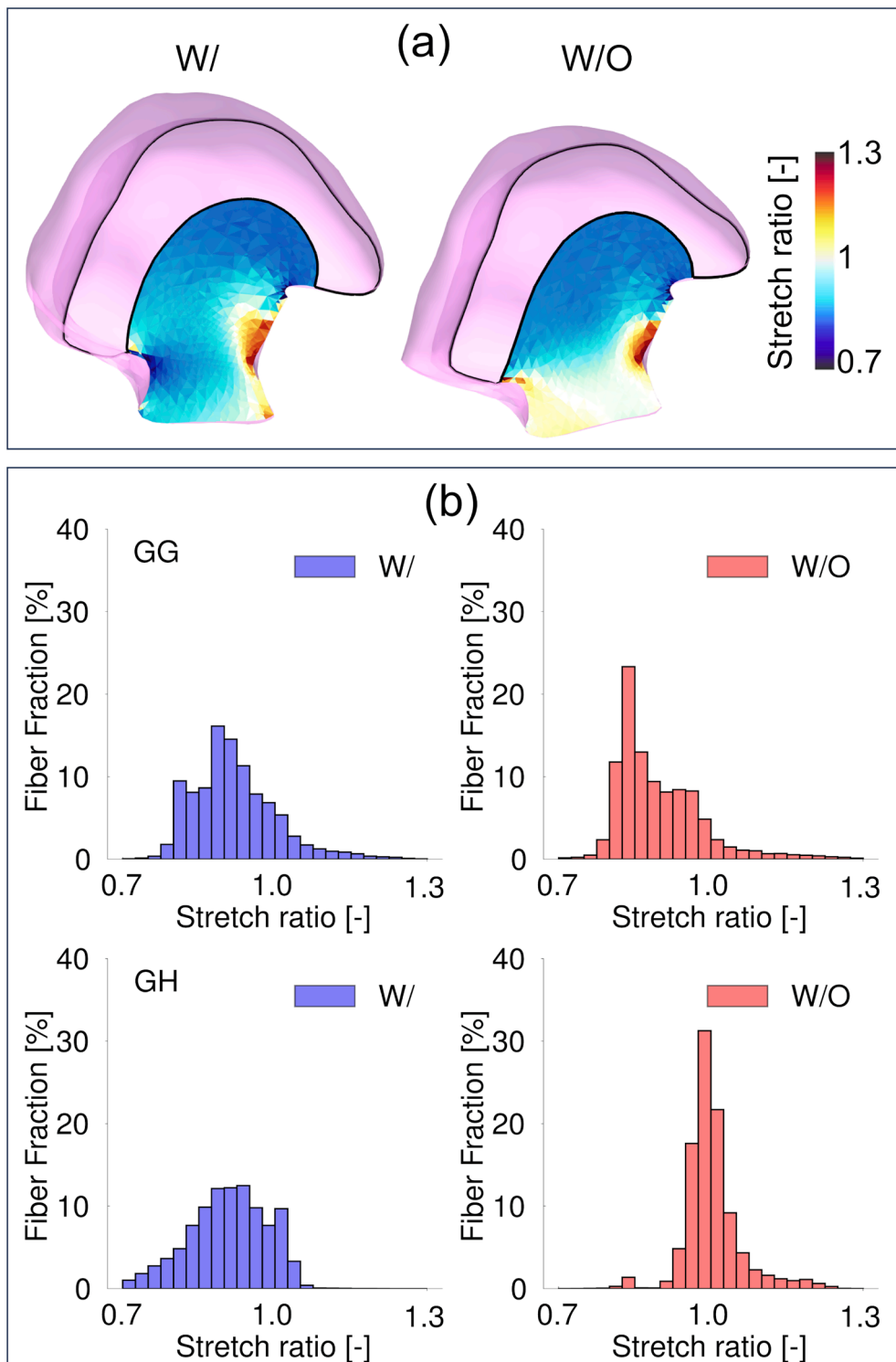


Fig. 5. (a) Spatial distribution of the fiber stretch ratio on the mid-sagittal plane and (b) volume fractions of the muscle fiber stretch ratio in the horizontal and oblique regions of the genioglossus (GG) and geniohyoid (GH) after tongue forward protrusion with/without hyoid bone movement.

the anterior direction. Thus, whole-tongue muscle effort should be considered in the production of actual tongue tip displacement in tongue forward protrusion. Fourth, computational simulation treated HB movement as prescribed motion, while these positions are determined by mechanical balances of suprathyroid and infrathyroid muscles. Although consideration of these surrounding muscles increases model complexities and redundancies of tongue motion, further detailed modeling involving these surrounding muscles could expand the application

ranges of the computational tongue model to further clarify the detailed mechanisms of tongue motor functions. Several studies successfully represented the HB movements by simplifying the suprathyroid and infrathyroid muscles as one-dimensional discrete elements (Kikuchi et al., 2023; Wu et al., 2014). These reasonable simplifications would be useful to simulate the tongue forward protrusion with considering the mechanical balances of the HB.

In conclusion, the current study investigated a kinematically

reasonable mechanism of tongue forward protrusion with consideration of HB movement using ultrasound imaging and subsequent computational simulation. Ultrasound imaging revealed HB displacement toward the anterior and superior directions with comparable ranges, whereas the tongue tip translated mainly toward the anterior direction. The computational simulation considering the HB movement described above demonstrated that the whole tongue body exhibited translation with HB movements and produced forward rotation because of the kinematic constraints of the GG. This rigid-like tongue motion enhanced tongue forward protrusion and increased the anterior displacement of the tongue tip by 1.5 times compared with the case without HB movement. Although the mechanism of tongue forward protrusion has been conventionally considered to be the anterior shift of the tongue body caused by contractions of GG lower (horizontal) region, the current results indicate that tongue forward protrusion can be understood as a combination of GG contraction and rigid-like tongue motion associated with HB movements caused by the suprathyroid and infrathyroid muscles. These findings may be useful for improving our understanding of the mechanism of the tongue forward protrusion, and suggest that not only the tongue muscles but also the suprathyroid and infrathyroid muscles associated with the HB movements have an impact on oral and speech mechanisms.

CRediT authorship contribution statement

Kyoichi Inoue: Writing – original draft, Visualization, Methodology, Investigation, Formal analysis. **Tomohiro Otani:** Writing – original draft, Supervision, Software, Project administration, Methodology, Investigation, Formal analysis, Conceptualization. **Kazunori Nozaki:** Writing – review & editing, Methodology, Funding acquisition, Data curation, Conceptualization. **Tsukasa Yoshinaga:** Writing – review & editing, Supervision, Methodology. **Shigeo Wada:** Writing – review & editing, Project administration.

Declaration of competing interest

The authors declare that they have no known competing financial interests or personal relationships that could have appeared to influence the work reported in this paper.

Acknowledgments

We thank Masahito Matsumura, Akihiro Fukuda, and Shun Takenaka for their technical contributions. This work was supported by research grants from JSPS Grants-in-Aid for Scientific Research (22H03438). We thank Benjamin Knight, MSc., from Edanz (<https://jp.edanz.com/ac>) for editing a draft of this manuscript.

Appendix A. Supplementary material

Supplementary data to this article can be found online at <https://doi.org/10.1016/j.biomech.2024.112445>.

References

Abd-El-Malek, S., 1939. Observations on the morphology of the human tongue. *J. Anat.* 73 (201–210), 3.

Al-Zanoon, N., Cummine, J., Jeffery, C.C., Westover, L., Aalto, D., 2024. The effect of simulated radiation induced fibrosis on tongue protrusion. *Biomech. Model. Mechanobiol.* <https://doi.org/10.1007/s10237-024-01860-4>.

American Speech-Language-Hearing Association, n.d. Orofacial Myofunctional Disorders (Practice Portal) [WWW Document]. URL www.asha.org/Practice-Portal/Clinical-Topics/Orofacial-Myofunctional-Disorders/ (accessed 20240619).

Bailey, E.F., 2011. Activities of human genioglossus motor units. *Respir. Physiol. Neurobiol.* 179, 14–22.

Behrman, A., Haskell, J., 2008. Exercises for voice therapy. Plural Publishing.

Buchaillard, S., Brix, M., Perrier, P., Payan, Y., 2007. Simulations of the consequences of tongue surgery on tongue mobility: implications for speech production in post-surgery conditions. *Int. J. Med. Robot.* 3, 252–261.

Buchaillard, S., Perrier, P., Payan, Y., 2009. A biomechanical model of cardinal vowel production: muscle activations and the impact of gravity on tongue positioning. *J. Acoust. Soc. Am.* 126, 2033–2051.

Dao, T.T., Tho, M.-C.-H.-B., 2018. A systematic review of continuum modeling of skeletal muscles: current trends, limitations, and recommendations. *Appl. Bionics Biomed.* 2018, 7631818.

Doran, G.A., Baggett, H., 1971. The genioglossus muscle: a reassessment of its anatomy in some mammals, including man. *J. Anat.* 110, 505.

Fujita, S., Dang, J., Suzuki, N., Honda, K., 2007. A computational tongue model and its clinical application. *Oral Sci. Int.* 4, 97–109.

Gomez, A.D., Elsaïd, N., Stone, M.L., Zhuo, J., Prince, J.L., 2018. Laplace-based modeling of fiber orientation in the tongue. *Biomech. Model. Mechanobiol.* 17, 1119–1130.

Gomez, A.D., Stone, M.L., Woo, J., Xing, F., Prince, J.L., 2020. Analysis of fiber strain in the human tongue during speech. *Comput. Methods Biomed. Eng.* 23, 312–322.

Hiemae, K.M., Palmer, J.B., 2003. Tongue movements in feeding and speech. *Crit. Rev. Oral Biol. Med.* 14, 413–429.

Kappert, K.D.R., Voskuilen, L., Smeele, L.E., Balm, A.J.M., Jasperse, B., Nederveen, A.J., van der Heijden, F., 2021. Personalized biomechanical tongue models based on diffusion-weighted MRI and validated using optical tracking of range of motion. *Biomech. Model. Mechanobiol.* 20, 1101–1113.

Kier, W.M., 2012. The diversity of hydrostatic skeletons. *J. Exp. Biol.* 215, 1247–1257.

Kikuchi, T., Michiwaki, Y., Azeami, H., 2023. Identification of muscle activities involved in hyoid bone movement during swallowing using computer simulation. *Comput. Methods Biomed. Eng. Imaging Vis.* 11, 1791–1802.

Kim, Y., McCullough, G.H., 2008. Maximum hyoid displacement in normal swallowing. *Dysphagia* 23, 274–279.

Koike, N., Ii, S., Yoshinaga, T., Nozaki, K., Wada, S., 2017. Model-based inverse estimation for active contraction stresses of tongue muscles using 3D surface shape in speech production. *J. Biomech.* 64, 69–76.

Kwan, B.C.H., Butler, J.E., Hudson, A.L., McKenzie, D.K., Bilston, L.E., Gandevia, S.C., 2014. A novel ultrasound technique to measure genioglossus movement in vivo. *J. Appl. Physiol.* 117, 556–562.

Laboissière, R., Ostry, D.J., Feldman, A.G., 1996. The control of multi-muscle systems: human jaw and hyoid movements. *Biol. Cybern.* 74, 373–384.

Moerman, K.M., Sprengers, A.M.J., Simms, C.K., Lamerichs, R.M., Stoker, J., Nederveen, A.J., 2012. Validation of continuously tagged MRI for the measurement of dynamic 3D skeletal muscle tissue deformation: Validation of continuously tagged dynamic 3D deformation measurement. *Med. Phys.* 39, 1793–1810.

Muto, T., Kanazawa, M., 1994. Positional change of the hyoid bone at maximal mouth opening. *Oral Surg. Oral Med. Oral Pathol.* 77, 451–455.

Otani, T., Kobayashi, Y., Tanaka, M., 2020. Computational study of kinematics of the anterior cruciate ligament double-bundle structure during passive knee flexion-extension. *Med. Eng. Phys.* 83, 56–63.

Pancher, H., Winnberg, A., Westesson, P.L., 1986. Masticatory muscle activity and hyoid bone behavior during cyclic jaw movements in man. A synchronized electromyographic and videofluorographic study. *Am. J. Orthod.* 89, 122–131.

Pittman, L.J., Bailey, E.F., 2009. Genioglossus and intrinsic electromyographic activities in impeded and unimpeded protrusion tasks. *J. Neurophysiol.* 101, 276–282.

Ross, C.F., Laurence-Chasen, J.D., Li, P., Orsbon, C., Hatsopoulos, N.G., 2024. Biomechanical and cortical control of tongue movements during chewing and swallowing. *Dysphagia* 39, 1–32.

Stavness, I., Lloyd, J.E., Payan, Y., Fels, S., 2011. Coupled hard–soft tissue simulation with contact and constraints applied to jaw–tongue–hyoid dynamics. *Int. J. Numer. Method Biomed. Eng.* 27, 367–390.

Sanders, I., Mu, L., 2013. A three-dimensional atlas of human tongue muscles: human tongue muscles. *Anat. Rec. (Hoboken)* 296, 1102–1114.

Stavness, I., Lloyd, J.E., Fels, S., 2012. Automatic prediction of tongue muscle activations using a finite element model. *J. Biomech.* 45, 2841–2848.

Takemoto, H., 2001. Morphological analyses of the human tongue musculature for three-dimensional modeling. *J. Speech Lang. Hear. Res.* 44, 95–107.

Webb, W.G., Adler, R.K., 2007. Neurology for the speech-language pathologist, 5th ed. Mosby, London, England.

Wei, K.-C., Hsiao, M.-Y., Wang, T.-G., 2022. The kinematic features of hyoid bone movement during swallowing in different disease populations: a narrative review. *J. Formos. Med. Assoc.* 121, 1892–1899.

Westbury, J.R., 1988. Mandible and hyoid bone movements during speech. *J. Speech Hear. Res.* 31, 405–416.

Wu, X., Dang, J., Stavness, I., 2014. Iterative method to estimate muscle activation with a physiological articulatory model. *Acoust. Sci. Technol.* 35, 201–212.

Yabunaka, K., Sanada, H., Sanada, S., Konishi, H., Hashimoto, T., Yatake, H., Yamamoto, K., Katsuda, T., Ohue, M., 2011. Sonographic assessment of hyoid bone movement during swallowing: a study of normal adults with advancing age. *Radiol. Phys. Technol.* 4, 73–77.

Zheng, L., Jahn, J., Vasavada, A.N., 2012. Sagittal plane kinematics of the adult hyoid bone. *J. Biomech.* 45, 531–536.